



Low-cost and high speed monitoring system for a multi-nozzle piezo inkjet head

Kye-Si Kwon^{a,*}, Yun-Sik Choi^a, Dae-Yong Lee^a, Jeong-Seon Kim^b, Dae-Sung Kim^b

^a Department of Mechanical Engineering, Soonchunhyang University, 646, Eupnae-ri, Shinchang-myeon, Asan-si, Chungnam 336-745, South Korea

^b SEMES Inc., Display Business Division, 278, Moshi-ri, Jiksan-eup, Seobuk-gu, Cheonan-si, Chungnam, South Korea

ARTICLE INFO

Article history:

Received 7 September 2011
Received in revised form 11 April 2012
Accepted 11 April 2012
Available online 21 April 2012

Keywords:

Piezo inkjet
Inkjet monitoring system
Piezo self-sensing

ABSTRACT

Inkjet technology has recently emerged as one of the most powerful patterning tools for manufacturing electronic devices. For inkjet technology to be a reliable patterning tool, the jetting status of inkjet dispensers needs to be monitored in order to detect jetting failures. We propose a new monitoring system that can show, within 2 s, the jetting status of a piezo driven inkjet head with 128 nozzles. For this purpose, a low cost monitoring module that can measure the piezo self-sensing signals was developed. The module consists of a detection circuit and a data acquisition (DAQ) system which can easily be integrated into existing printing systems. In addition, a software algorithm is presented to demonstrate the effectiveness of the proposed method when it is applied to inkjet-based manufacturing systems.

© 2012 Elsevier B.V. All rights reserved.

1. Introduction

The application of inkjet technology has broadened from desktop printers to become a manufacturing tool for electronic devices such as large area display applications, radio frequency identification (RFID), and printed circuit boards (PCBs) [1–3]. To ensure manufacturing productivity and reliability, any problems in jetting performance must be identified and fixed immediately. As a result, there is significant demand for an improved system to monitor jetting status during the printing process [1,4–9].

Vision-based methods using charge-coupled device (CCD) cameras have been utilized to monitor jetting status since jetting behavior can be easily understood using images [1,10,11]. However, such methods require precise mechanical alignment of the camera with respect to the nozzle of interest. One major drawback of vision-based monitoring is that it takes a significant amount of time to scan all nozzles when monitoring a multi-nozzle head.

The use of piezo self-sensing in an inkjet head has recently drawn attention as an alternative to vision based monitoring [4–9]. A piezo inkjet head uses a piezo actuator to jet ink droplets. On the other hand, the piezo actuator can be used as a sensor by sensing the force that results from the pressure wave inside the inkjet dispenser. Due to these features, the sensing signals (or self-sensing signals) from a piezo actuator in an inkjet head can be used to monitor the jetting status of the inkjet head. Since the first research paper

on air-bubble detection by Jong et al. [5], the feasibility of using piezo self-sensing signals to detect jetting failures has been discussed in the literature [6–9]. Jong et al. used a changeover switch for selecting the required function of the piezo, (i.e., as either a sensor or an actuator) to detect air bubbles entrapped in the inkjet head [5]. Similar approaches using changeover switches to monitor the inkjet head's operational conditions have already been described in patents by Simons and Groninger [6]. Recently, a method using a bridge circuit was developed to detect inkjet malfunctions [4]. However, few published studies have dealt with practical problems that occur when the technology is used to monitor a multi-nozzle head. Note that most inkjet printheads have many nozzles, and the monitoring method and detection algorithm should be optimized accordingly. A method for monitoring a multi-nozzle head was presented in our previous study [8]. However, the measurement scheme and algorithm were not optimized. As a result, the monitoring speed was too slow for practical application.

In this study, we will focus on the measurement circuit and data processing algorithm to monitor a multi-nozzle head. To overcome the previous shortcomings, we developed a high speed monitoring module that can be easily integrated into existing printheads. The cost of the monitoring module was minimized by simplifying the hardware such that only one analog input channel of a data acquisition (DAQ) system was required to monitor 128 nozzles. Also, the scanning time required for data acquisition of all the nozzles was minimized by means of a scenario-based jetting and measurement algorithm. A software program is presented to allow the jetting status of a multi-nozzle head to be understood at a glance. Using this software, one can compare the self-sensing results with vision-based measurements for verification. To understand the

* Corresponding author. Tel.: +82 41 530 1670; fax: +82 41 530 1550.

E-mail address: kskwon@sch.ac.kr (K.-S. Kwon).

URL: <http://inkjet.sch.ac.kr/> (K.-S. Kwon).

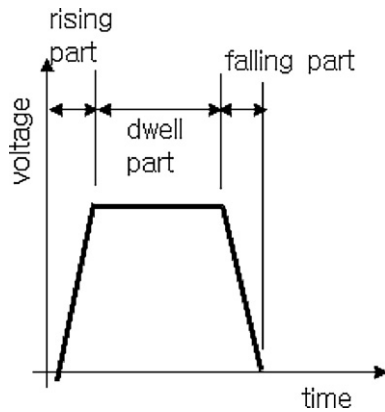


Fig. 1. Driving waveform for piezo inkjet head.

jetting conditions of all nozzles, the deviation of monitoring signals from the reference signal of each nozzle is represented in a bar graph.

2. Piezo self-sensing measurement methods

2.1. Monitoring the inkjet head using piezo self-sensing

The jetting of ink from an inkjet printhead can be subject to malfunctions caused by air bubbles entrapped in the dispensers, ink wetting on a nozzle's surface, nozzle clogging due to particles in the ink, or ink drying on the nozzle's surface [4]. Among these malfunctions, air-bubbles trapped in the inkjet head are known to be a major problem since the air bubbles can be generated even during drop formation [5,12,13]. To detect jetting failure related to entrapped air bubbles, the use of a piezo self-sensing signal has been shown to be effective [4]. The capabilities and limitations of the self-sensing signals to detect jetting failures due to other causes such as nozzle wetting and particle clogging need to be investigated; however, this is beyond the scope of this study. The primary focus was the measurement methods and a detection algorithm necessary for monitoring inkjet printheads based on the piezo self-sensing signal.

When a driving voltage (Fig. 1) is used to drive piezo actuators in an inkjet head, the rising portion of the voltage waveform results in contraction of the piezo actuator, whereas the falling part produces an expansion. Piezo actuation generates a pressure wave in the ink. Proper driving voltage amplifies the pressure wave such that a droplet of ink can be jetted from the inkjet head. The relationship between jetting performance and the driving voltage waveform was discussed in detail in [14,15]. The residual pressure wave of the ink remains until it is damped out, even after the droplet is jetted. If the jetting condition changes, the propagation of the pressure wave inside the head will change accordingly. Thus, the pressure wave can be a good indicator of whether jetting conditions are acceptable.

It is well known that a piezo device can be used as both a sensor and an actuator. There are two components in the measured piezo current [4]:

$$i = i_q + i_c \quad (1)$$

where $i_c = C(dV/dt)$ and $i_q = \kappa(dq_p/dt)$. Here, i_q results from the piezo-electric charge due to the change of the piezo-strain, and i_c is the powering current that results from the applied voltage behaving as a capacitor with capacitance C . The current component related to i_q , which contains information on the pressure wave inside the head, is referred to as a self-sensing signal. Therefore, current i can be used

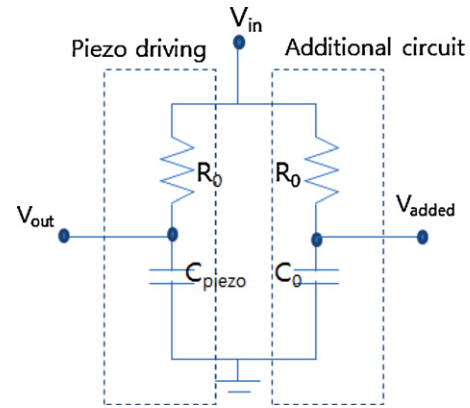


Fig. 2. Bridge circuit for piezo self-sensing.

to monitor inkjet jetting conditions by extracting the self-sensing signal from the measured piezo current [4,15].

2.2. Detection circuits for a multi-nozzle head

To measure the self-sensing signal from an inkjet head with a single nozzle, a bridge circuit was used in [4]. Fig. 2 shows a typical bridge circuit for this purpose. An equivalent capacitor, C_0 , with the same capacitance as piezo capacitance, C_{piezo} , in the printhead should be used in the bridge circuit. By using the bridge circuit, the powering current component due to the piezo capacitance can be effectively removed by subtracting voltage V_{added} from V_{out} , where V_{out} is the output voltage from the piezo driving circuit, and V_{added} is the voltage from the added circuit.

When monitoring multi-nozzle heads, this bridge circuit cannot be used directly. Specifically, the measurement circuit and method should differ according to the driving scheme for a multi-nozzle head. Methods for driving a multi-nozzle head include a drive per nozzle (DPN) method shown in Fig. 3(a); and a shared driver method shown in Fig. 3(b).

One merit of the DPN driving scheme is that the jetting performance of each nozzle can be controlled independently. However, there are cost issues since one driver is required for each nozzle. Similar to the DPN driving scheme, a piezo self-sensing signal at each nozzle can be measured independently [9]. In this case, the number of circuits and DAQ channels was the same as the number of nozzles in order to measure each piezo current. The method might not be practical for use in industry because of an issue regarding the cost of the measurement hardware.

As an alternative method to the DPN driving scheme, a shared driver can be used to drive a group of nozzles in a multi-nozzle printhead as shown in Fig. 3(b), which would serve to reduce the cost and complexity of the driver electronics. Due to the simplicity of its driving hardware, the driving method based on shared drivers is more commonly used in practice unless jetting uniformity among nozzles is a critical issue. Thus, we focused on developing a monitoring method for a multi-nozzle head that uses the shared driving scheme as shown in Fig. 3(b). To extract the self-sensing signal, the current in the piezo actuator is measured on the shared driving line. The current measurement on the shared line can reduce hardware costs since the number of DAQ channels and detection circuits is reduced. However, we note that the measured self-sensing signals from jetting nozzles can become mixed due to simultaneous jetting of multiple nozzles. Thus, jetting status monitoring based on current measurements of the shared line may not be possible during actual printing, where more than one nozzle must be actuated simultaneously. Therefore, the monitoring process needs to be performed between printing passes as shown in Fig. 4. Alternatively,

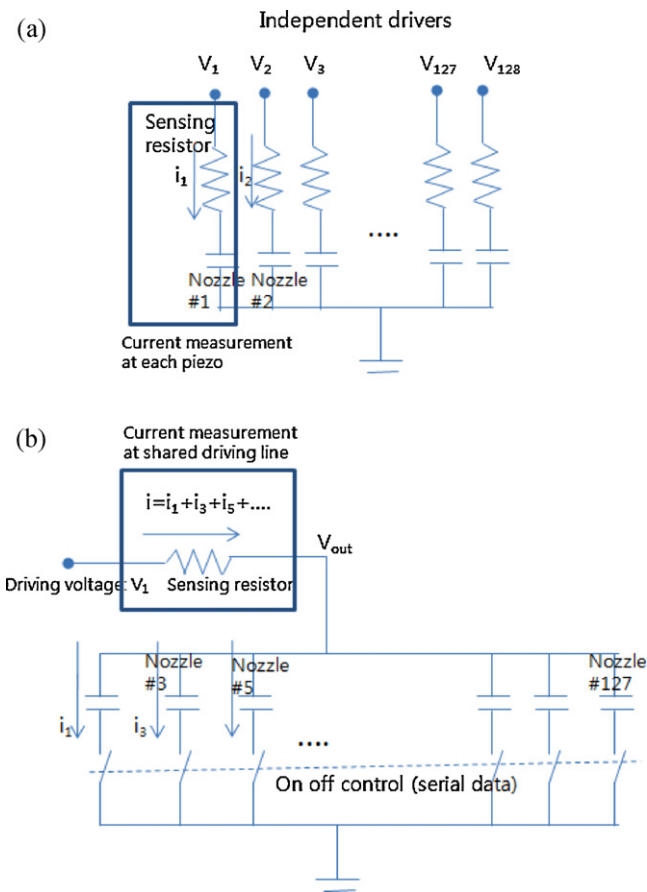


Fig. 3. Inkjet printhead driving schemes: drive per nozzle (DPN) and (b) shared driver (for odd nozzle).

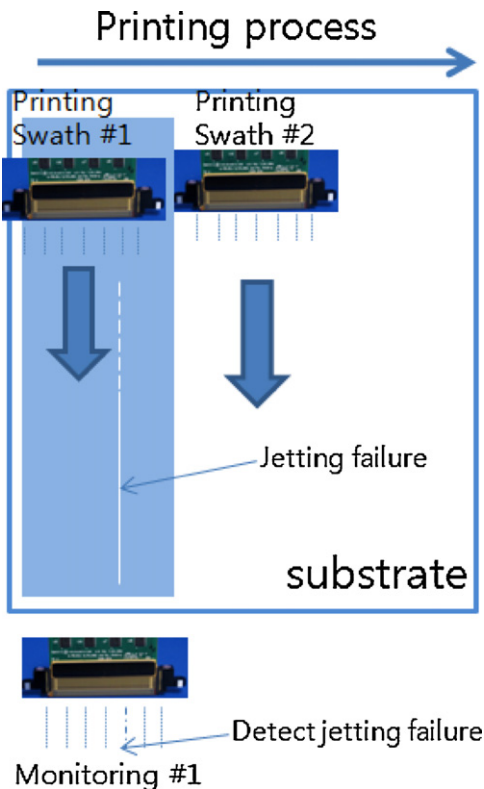


Fig. 4. Monitoring scheme during printing process.

the monitoring process could be performed upon completion of printing an image prior to the next printing. The process requires extra time to monitor the inkjet head, which in turn increases the total time needed for printing. Therefore, to increase manufacturing productivity, the reduction of monitoring time is one of the key technical problems to be solved.

To examine such practical issues, a commercial multi-dispenser inkjet printhead (SL-128, Dimatix, USA) was used for this study. The printhead uses two shared drivers for 128 nozzles: one driver is used for driving the odd-numbered nozzles as shown in Fig. 3(b), and the other driver is used for the even-numbered nozzles. Fig. 5 shows the conventional driving scheme for the multi-nozzle head. To drive the inkjet head, both the waveform voltage and the nozzle on-off information are transferred to the pattern generator prior to jetting. Then, a driver is used to amplify the waveform signal for driving the printhead.

To obtain piezo self-sensing signals, electronic circuits to measure the piezo current must be inserted between the driver and inkjet head. Also, the bridge circuit should be modified to use the shared driving line to measure current and extract the self-sensing signals from the SL-128. However, the additional circuits for a bridge circuit, which was required to be connected in parallel to the existing inkjet head driving circuits, could lead to additional driving current. This might cause distortion in the actual driving voltage and affect the jetting performance. In previous work, a sensing method for the multi-nozzle head (SL-128) was developed to avoid the additional current [8]. For this purpose, an additional driving voltage V_{ref} was used to drive an additional circuit with an equivalent capacitor. However, another problem arises in that the additional driver increases cost and might not be desirable in a practical inkjet system. Furthermore, two analog input channels for data acquisition were used in [8], even though simultaneous two channel data acquisitions are not required since only one nozzle is selected at a time for monitoring.

To overcome previous shortcomings, we developed a new detection circuit and DAQ system in the form of a circuit module, as shown in Fig. 6. The measuring circuit and DAQ hardware were optimized such that the number of circuits could be reduced from two to one, as shown in Fig. 7. Also, the number of drivers was reduced by removing the additional driver. In this new version, the additional equivalent capacitors needed to form a bridge circuit were not used. As a result, additional current to drive the equivalent capacitor was not required. Another advantage of the proposed method is that an easily integrated module-based circuit hardware is used. For easy insertion of the module in the driving circuit, we developed an adaptor that has a sensing resistor R_0 to measure current, as shown in Fig. 7. In this manner, the voltage corresponding to the self-sensing components can be extracted from the drive voltage lines for odd and even nozzles, V_{1out} and V_{2out} , which is shown in Fig. 7. Note that the sensitivity of the self-sensing signal can be adjusted by selecting proper sensing resistor impedances. To extract the self-sensing component effectively, a detection circuit consisting of a differential amplifier and analog filters was developed such that V_{2out} can be subtracted from V_{1out} . The input impedance of the circuit was designed to be large (about $1\text{ M}\Omega$) so that the driving voltages V_{2out} and V_{1out} would have less chance of being affected by the measurement circuit. By using direct subtraction of two signals V_{1out} and V_{2out} , as shown in Fig. 7, an additional circuit with an equivalent capacitor C_0 is not required, unlike a conventional bridge circuit. In addition, the number of DAQ channels can be reduced from two to one since there is only one voltage output in the developed circuit.

The measured current is a summation of all the currents of the jetting nozzles connected to the driving line. Therefore, to identify the jetting status of a specific nozzle, the nozzle needs to be jetted for monitoring with the other nozzles turned off. For a

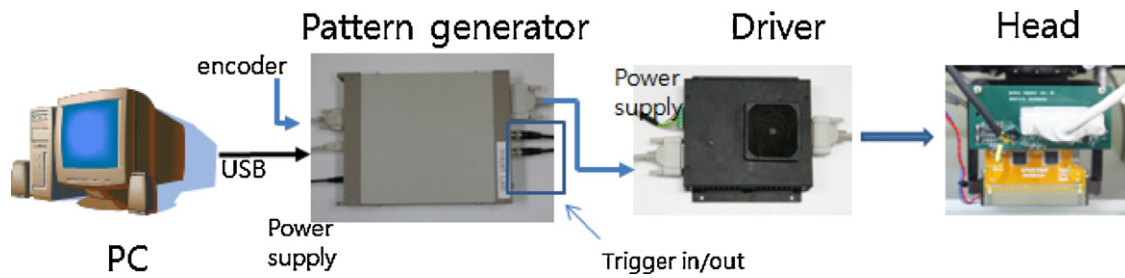


Fig. 5. Driving scheme for typical multi-nozzle inkjet head.

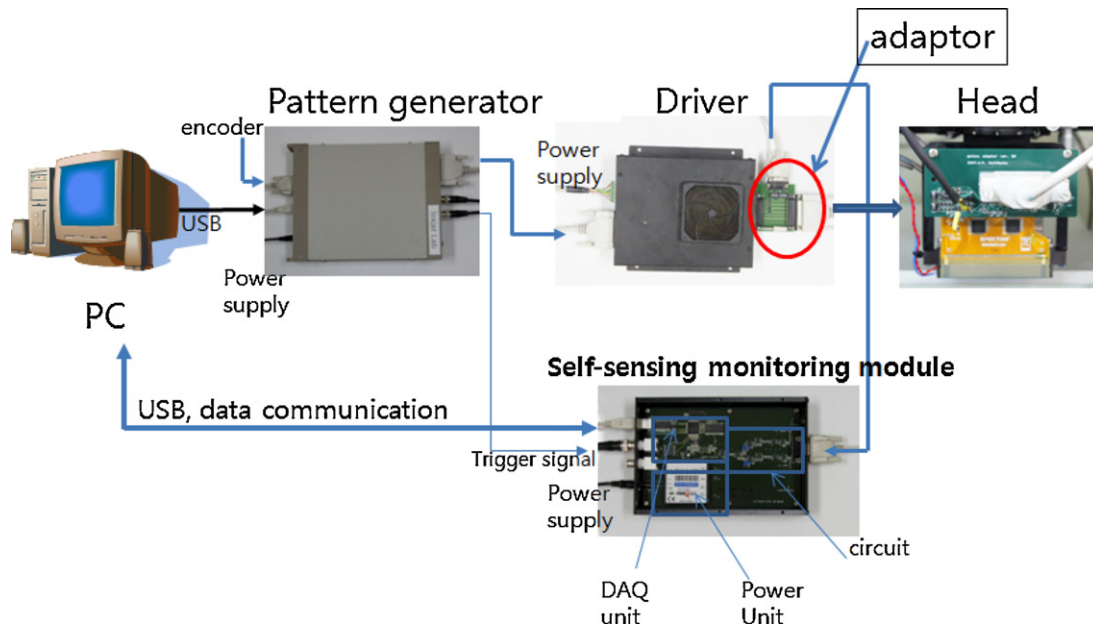


Fig. 6. Monitoring system for inkjet head using a developed monitoring module.

better explanation of the proposed method, we used the example of monitoring nozzle number 3 without loss of generality. To monitor nozzle number 3, only nozzle number 3 needs to be in jetting condition. In this case, the measured voltage $V1_{out}$ can be written as

$$V1_{out} = V1_{in} - R0i_{odd} = V1_{in} - R0i_3 - R0i_3 = V1_{in} - R0 \left(C_3 \frac{dV1_{out}}{dt} + \kappa \frac{dq_3}{dt} \right) \quad (2)$$

where i_{odd} is the summation of all currents in the odd nozzles; i.e., $i_{odd} = i_1 + i_3 + i_5 + \dots + i_{127}$. When only driving nozzle 3, the relationship $i_{odd} = i_3$ holds. Here, i_3 and C_3 are the current and capacitance of the piezo actuator in nozzle number 3, respectively, and $V1_{in}$ is the driver output voltage for the odd nozzle. As defined by Eq. (2), the self-sensing voltage component $R0(\kappa(dq_3/dt))$ associated with nozzle number 3 can appear in the output voltage $V1_{out}$. It should

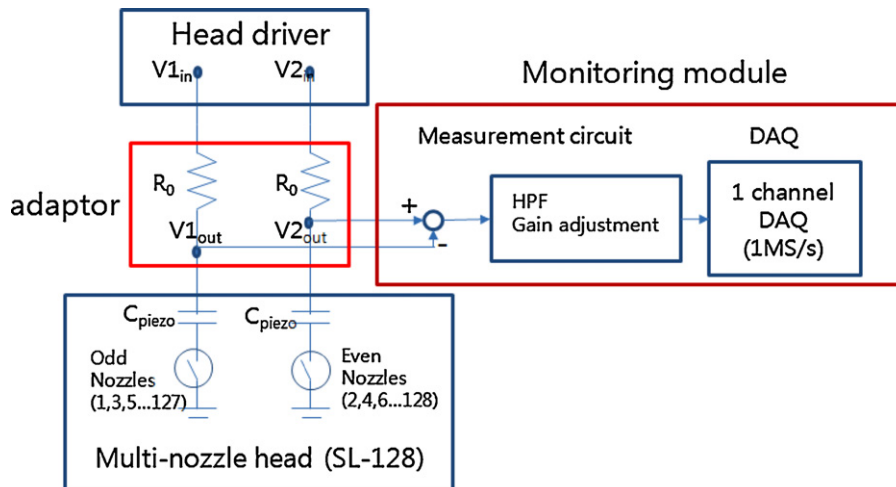


Fig. 7. Schematic of measurement circuit.

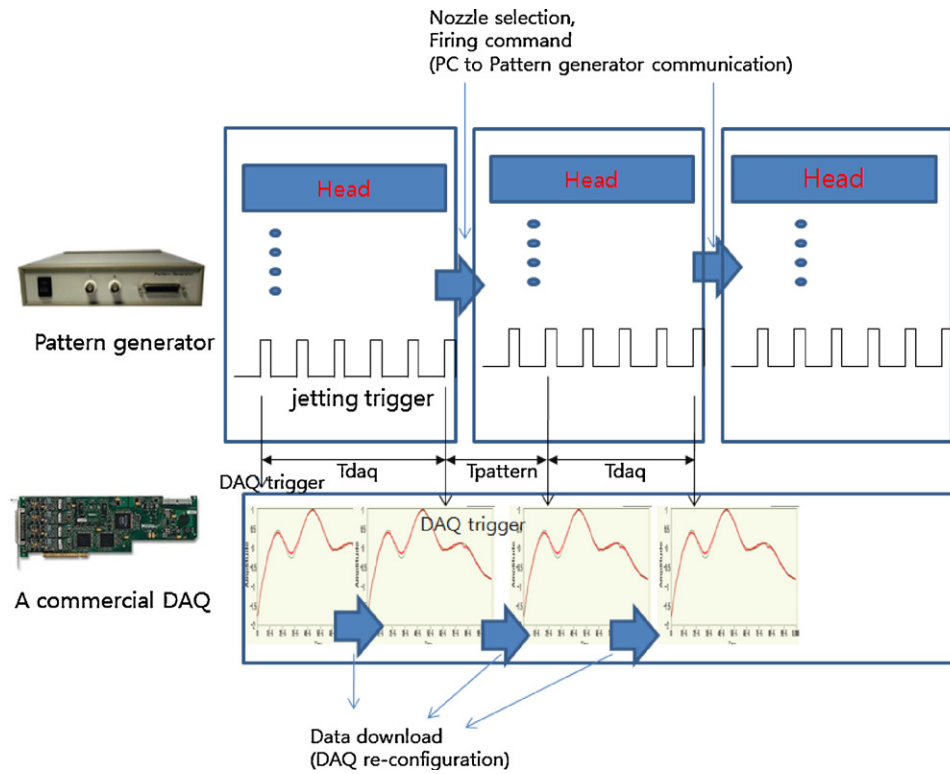


Fig. 8. Monitoring scheme using conventional DAQ system.

be noted that if R_0 becomes small, the voltage component due to the self-sensing component decreases, and vice versa. However, if R_0 is increased for the sake of higher sensitivity to the sensing signal, the jetting performance will be affected due to its influence on the actual driving voltage. In effect, there are tradeoffs between sensing capability and jetting performance. Considering both, a resistance of dozens of ohms for R_0 is recommended. The voltage related to the self-sensing component $R_0(\kappa(dq_3/dt))$ can be as small as 1/1000 of the input voltage V_{1in} . As a result, the self-sensing component is difficult to observe from measurement of V_{2out} or V_{1out} unless the voltage is magnified. On the other hand, there is no self-sensing component in V_{2out} when all the even nozzles are turned off, i.e., $i_{even} = 0$. Thus,

$$V_{2out} = V_{2in} - Ri_{even} = V_{2in} \quad (3)$$

Here, the driving voltage V_{2in} for even nozzles normally has the same waveform shape as the driving voltage for odd nozzles V_{1in} (i.e., $V_{1in} = V_{2in}$). In order to extract sensing signal $x_3(t)$ from the measured V_{1out} , a differential amplifier was used to subtract V_{2out} from V_{1out} as follows:

$$x_3(t) = G(V_{2out}(t) - V_{1out}(t)) \approx G \left[R_0 \left(C_3 \frac{dV_{1out}}{dt} + \kappa \frac{dq_3}{dt} \right) \right] \quad (4)$$

Here, the gain G is needed for proper amplification of the signal to measure the voltage via data acquisition. The signal $x_3(t)$ will be similar to a conventional bridge circuit signal since the large driving voltage V_{1in} can be removed. The bridge circuit has been used to eliminate the unchanged nominal signal thus maximizing piezo self-sensing signal [4]. Note that there can be an additional voltage component in the measured voltage $x_3(t)$. The first part of the sensing signal in Eq. (4) $R_0(C_3(dV_{1out}/dt))$ is less affected by the inkjet status, whereas the voltage related to the self-sensing component $R_0(\kappa(dq_3/dt))$ is directly related to the jetting status. The proposed method for detecting inkjet malfunctions uses post-processing of the sensing signal, i.e., subtraction of the monitored signal from the reference signal. During the process, the signal

component less related to the self-sensing signal $R_0(C_3(dV_{1out}/dt))$ will be canceled out, and only the variation of the self-sensing component due to a jetting status change will be detected. This will be further discussed in Section 3.1.

Since the proposed method uses a differential amplifier that subtracts V_{2out} from V_{1out} to extract the self-sensing signal, the signal measured from even nozzles will have opposite signs compared to the signal measured from odd nozzles. Assuming that only one of the even nozzles is in a jetting state, measured signals for an even nozzle can be obtained from the developed circuit as follows:

$$x_n(t) = \frac{G}{10}(V_{2out}(t) - V_{1out}(t)) \approx -\frac{G}{10} \left[R_0 \left(C_n \frac{dV_{2out}}{dt} + \kappa \frac{dq_n}{dt} \right) \right] \quad (5)$$

$$n = 2, 4, 6, \dots, 128$$

Here, $V_{1out} = V_{1in}$ holds because there is no current in odd nozzles for the case of monitoring an even nozzle. However, in practice, we note that signals from even nozzles $x_i(t)$, $i = 1, 3, 5, \dots, 127$, do not have perfectly opposite signs with respect to the signals from odd nozzles $x_i(t)$, $i = 2, 4, 6, \dots, 128$, since it is difficult to cancel out V_{1in} (or V_{2in}) from V_{1out} (or V_{2out}) via differential circuits. Experimental results related to extracting the self-sensing signal will be discussed in Section 3.1.

2.3. Data acquisition systems for high speed monitoring

Data acquisition of self-sensing signals is needed because the measured signals must be processed further to determine if the corresponding nozzles have malfunctioned. The method for data acquisition should be optimized since it is closely related to the amount of time needed to monitor the total print head status.

To acquire the self-sensing signals, we must consider a proper DAQ system with regard to the number of analog input channels, the sampling rate, and the number of sampled data values per acquisition. Considering the fundamental frequency of the self-sensing signal (dozens of kHz), the sampling rate for the DAQ

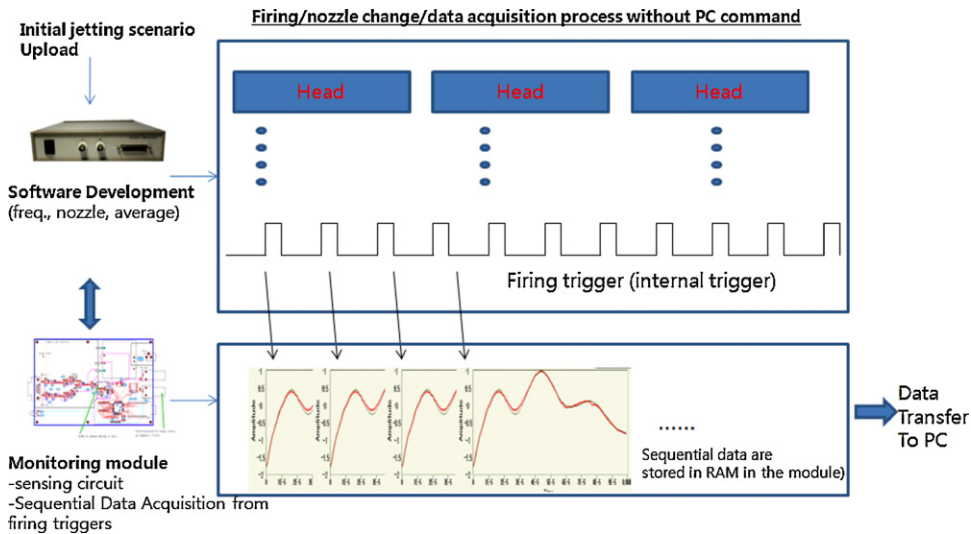


Fig. 9. High speed monitoring scheme using developed monitoring module.

system should be at least 1 mega-sample per second (1 MS/s). The time span for monitoring should be at least 100 μ s to monitor jetting behavior. At least 100 self-sensing data samples per acquisition will be needed to monitor the self-sensing signal behavior if the sampling rate for data acquisition is set to 1 MS/s. The data acquisition for self-sensing signals was synchronized with respect to the jetting trigger signal. The synchronization of data acquisition with respect to the jetting trigger is important because the same starting signal is needed for data averaging to reduce the electrical noise. Also, a direct comparison of measured signals requires the synchronization to detect possible malfunctions. This will be further discussed in Section 3.1.

A commercial DAQ system (PCI-6110, National Instrument, USA), which has sampling rate capability of up to 5 MS/s, was used in our previous work [8]. Fig. 8 illustrates a measurement scheme using the commercial DAQ system. The two analog input channels of the DAQ system were used to measure output voltages from two driving (or sensing) circuits described in [8]. However, as in most conventional DAQ systems, the measurement is based on acquiring and processing the sensing data before the next data acquisition. As a result, the time T_{daq} was required between two acquisitions. This was due to the re-configuration of the DAQ for the next acquisition and data download to the PC for further data processing when a conventional DAQ system was used. In addition, re-configuration of the pattern generator to select the nozzle for jetting was required because the measurement scheme was based on monitoring one nozzle at a time. Jetting nozzle selection requires communication between the computer and the pattern generator via USB, and takes time $T_{pattern}$. Considering these time requirements, the total time for the measurement process can be estimated from

$$T_{\text{monitoring}} = N_{\text{ave}} \times T_{\text{daq}} \times N_{\text{nozzle}} + N_{\text{nozzle}} \times T_{\text{pattern}}, \quad (6)$$

where N_{ave} is the number of averaged signals from a nozzle and N_{nozzle} is the number of nozzles to be scanned. It is difficult to measure T_{daq} and T_{pattern} exactly, but we can understand their effect by measuring the total monitoring time $T_{\text{monitoring}}$. The total time required to monitor a printhead with 128 nozzles was measured to be about 10 s using the conventional DAQ system described in [8]. However, a scanning time of 10 s might be too slow to be used in practice. Nonetheless, the required time to monitor 128 nozzles using the self-sensing signal was much shorter compared to vision-based measurements, which took more than 2 min to scan 128 nozzles.

To reduce the monitoring time, we propose a new measurement scheme to replace the conventional measurement approach. In the new scheme, the data acquisition method and nozzle selection scheme were optimized. For example, all of the test conditions including monitoring nozzles and the number of data acquisitions were pre-set prior to the monitoring process. This was done by initially uploading the jetting scenario in the pattern generator and DAQ system. As a result, there was no need for PC communication between the computer and pattern generator (or DAQ system) for re-configuration during the monitoring process. Using the proposed method, the jetting nozzle can be changed between consecutive trigger signals that are internally generated at a frequency (for example, 5 kHz) from the pattern generator. A similar scheme has been used for bitmap image printing, in which jetting information from each nozzle is uploaded to a pattern generator prior to printing. Thus, the development of a software algorithm is needed rather than a hardware modification of the pattern generator. Note that the jetting trigger is generated internally from the pattern generator's internal frequency generator used primarily for monitoring purposes unlike in printing applications. In the case of printing application, encoder signals for motion control (or external triggers) are used as the jetting triggers. The jetting scenario should be incorporated with data acquisition such that all the jetting triggers can be used for data acquisition. For this purpose, hardware for the DAQ system was developed such that the self-sensing signals were acquired at each jetting trigger, and each acquired data item was temporarily stored in the random access memory (RAM) of the DAQ system. After acquiring self-sensing signals of all nozzles based on the jetting scenario, all data stored in the RAM were downloaded to the PC for further data processing. By developing a DAQ system based on the proposed method, the monitoring speed can be reduced significantly, unlike previous methods. The developed DAQ scheme was integrated into the monitoring module in which the developed sensing circuit is located. The DAQ sampling rate was 1 MS/s and 1 Mbytes of RAM was used in the DAQ system. The configuration of the DAQ and data transfer to the computer were implemented over universal serial bus (USB) between the computer and monitoring module.

Fig. 9 illustrates the inkjet head monitoring system developed to maximize scanning speed. Note that the scanning time is only related to jetting frequency and the number of data averagings. The time required to scan the entire nozzle is given by

$$T = \frac{N_{\text{ave}} \times N_{\text{nozzle}}}{\text{frequency}} \quad (7)$$

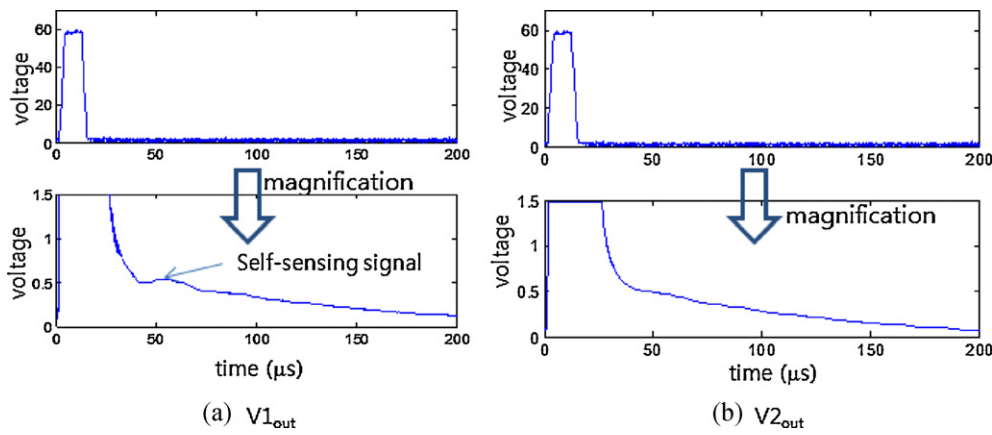


Fig. 10. Measured actual driving voltages (nozzle number 3 is in jetting condition).

For example, assuming that the jetting frequency is 5 kHz and the averaging number is 10 for each nozzle, then it will take only 0.256 s to scan 128 nozzles. Thus, the scanning time for the entire nozzle is fast enough to be performed during the printing process on a regular or irregular basis without a major interruption of the printing process. However, it will take an additional 1 or 2 s to calculate the measured signals and show the results in an effective way. This time requirement is mainly related to computer speed and much faster results are expected in the near future as computer speed advances.

For high throughput in manufacturing, more than one head is commonly used. In such a case, a number of self-sensing modules for each inkjet heads can be installed. Each monitoring module can acquire the sensing signals from each head independently. Thus, the total scanning time for monitoring more than one head will not increase significantly compared to single head monitoring but, computation time to process the acquired sensing signals may increase slightly.

3. Experiments

3.1. Jetting failure detection algorithm

To monitor jetting status, the proposed algorithm needs a reference signal for comparison with the monitored self-sensing signal. To detect a jetting failure, the reference signal should represent the normal jetting condition and must be measured prior to the monitoring process. The monitored self-sensing signal is then measured to determine jetting status by comparing it to the reference signal. The jetting status of nozzle number k can be judged by V_k in Eq. (8), which is the sum of the squared difference between the reference signal and monitored signal as follows:

$$V_k = \sum_{j=1}^N [x_k^r(j) - x_k^m(j)]^2 \quad (8)$$

Here, super-scripts r , m , and N represent reference signal, monitored signal, and number of sampled self-sensing data, respectively. By using this equation, the powering current component ($C_n(dV_{2out}/dt)$ or $C_n(dV_{1out}/dt)$) will be canceled out, and only the difference of self-sensing signals compared to the reference signal are effectively measured. Then, V_k is compared to a threshold value. If V_k exceeds the threshold value, the nozzle number k can be classified as abnormal. Proper selection of the threshold value is important. If the threshold value is small, then the normal condition can potentially be classified as abnormal. If the threshold value is large, then only severe nozzle conditions can be detected, thus

ignoring minor malfunctions. Note that the direct subtraction of two signals using Eq. (8) may lead to inaccurate monitoring results due to electrical noise in the measured signals. Averaging of the data was used to increase detection accuracy by averaging out noise, even though it increases monitoring time. Digital filtering of the measured signals is also required to suppress low frequency drift and high frequency noise prior to using Eq. (8).

For a better explanation, consider a case in which the experimental data from the developed circuit shown in Fig. 7 is used to measure the self-sensing signal from a Dimatix SL-128 multi-nozzle head. To drive the inkjet head, the typical waveform shown in Fig. 1 is used. Here, the rising/falling time and dwell time are set to 3 µs and 9 µs, respectively. Model fluid (XL-30, Dimatix) was used as the jetting fluid. The temperature of the head was held at 30 °C to maintain proper jetting of the fluid. A waveform with a magnitude of 60 V was applied for ink jetting. Fig. 10 shows the measured values of V_{1out} and V_{2out} when only nozzle number 3 was in a jetting status, with the other nozzles turned off. Since the self-sensing component voltage was very small compared to V_{in} , the effect of the piezo self-sensing component was difficult to observe without amplification, as shown in Fig. 10(a). Note that V_{2out} does not have a self-sensing component as a result of no piezo actuation in the even numbered nozzles, as shown in Fig. 10(b).

As previously discussed, the self-sensing signal can be effectively extracted by subtracting V_{2out} from V_{1out} . Fig. 11 shows the measured output voltage from the circuit in Fig. 7. The measured signal will change according to the jetting status, and jetting failure can be detected by comparison of the monitored self-sensing

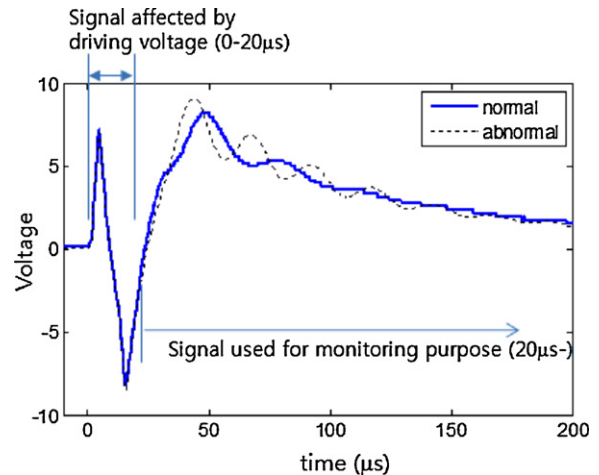


Fig. 11. Comparison of two signals, $x_3^r(t)$ and $x_3^m(t)$, measured at normal and abnormal jetting conditions, respectively.

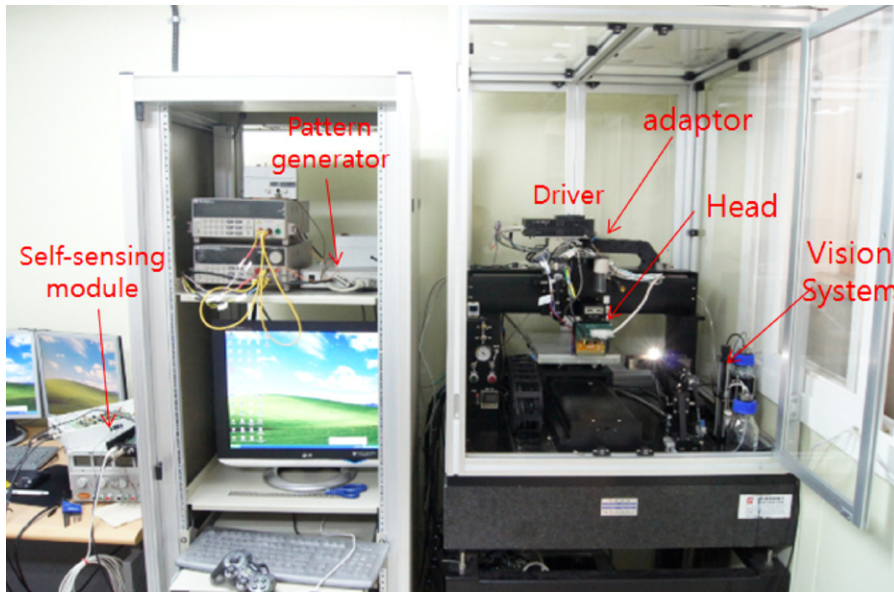


Fig. 12. Laboratory developed printing system.

signals with the reference signals. If the self-sensing signal differs significantly from the reference signal as shown in Fig. 11, the corresponding nozzle is diagnosed as a misfiring nozzle. Note that the first part of the extracted signal (0–20 μs) is likely to be influenced by the driving voltage as well as by the powering current component, which are not related to jetting conditions. Therefore, the first parts of the self-sensing signals (0–20 μs) were excluded in this study.

3.2. Detection software and experimental results

For a demonstration of the proposed method, the monitoring module was integrated into the laboratory-developed printing system as shown in Fig. 12 [16]. The printing system has a drop watcher module to visualize droplet images. To observe a droplet image from a specific nozzle, linear stages were used for position control. To visualize the jetting from the nozzle by stroboscopic means, a CCD camera and light-emitting diode (LED) light were used. Two trigger pulse signals were generated from two counters (PCI-6110, National Instrument, USA). One digital pulse was used to

generate trigger signals for ink jetting. The other digital signal was used to control the light-emitting diode (LED) light for strobed droplet images. The two signals were synchronized, and the delay time between the two trigger signals was controlled to obtain frozen droplet images. The measurement method for the droplet image was discussed in our previous works [10,11]. By using the drop watcher, the jetting condition can be visualized and compared with monitored results based on piezo self-sensing signals.

As discussed in Section 3.1, the proposed method uses the self-sensing signal measured under normal jetting conditions as reference data. Note that groups of nozzles may have similar reference signals. However, some nozzles could have different reference signals. So, it is recommended that each nozzle have its own reference data. It is critical to obtain the reference data of each nozzle to truly represent normal jetting conditions. To ensure normal jetting conditions, the droplet jetting speed was measured using a vision-based method to determine whether the jetting status was normal. The method used to measure jetting speed is described in [10]. From the measured jetting speed, nozzles with normal jetting conditions can be identified by setting the acceptable range of jetting speeds

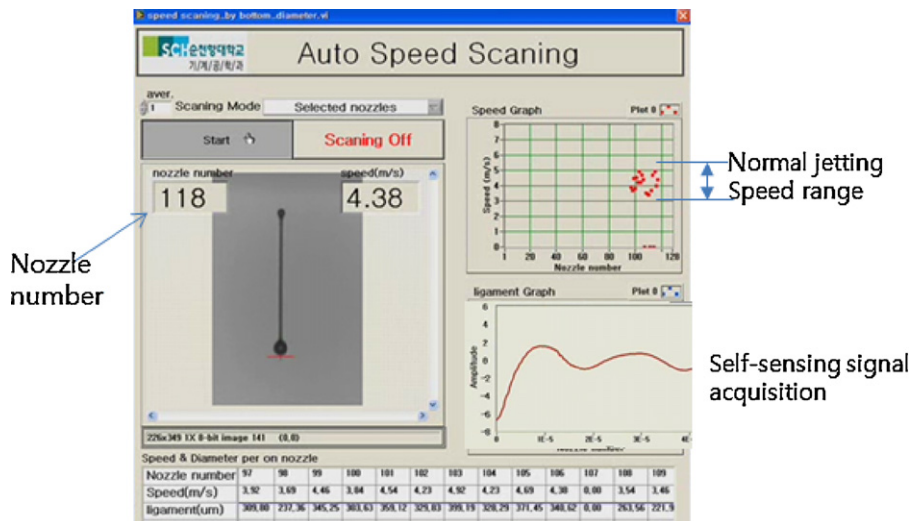


Fig. 13. Speed scanning for defining normal jetting conditions.

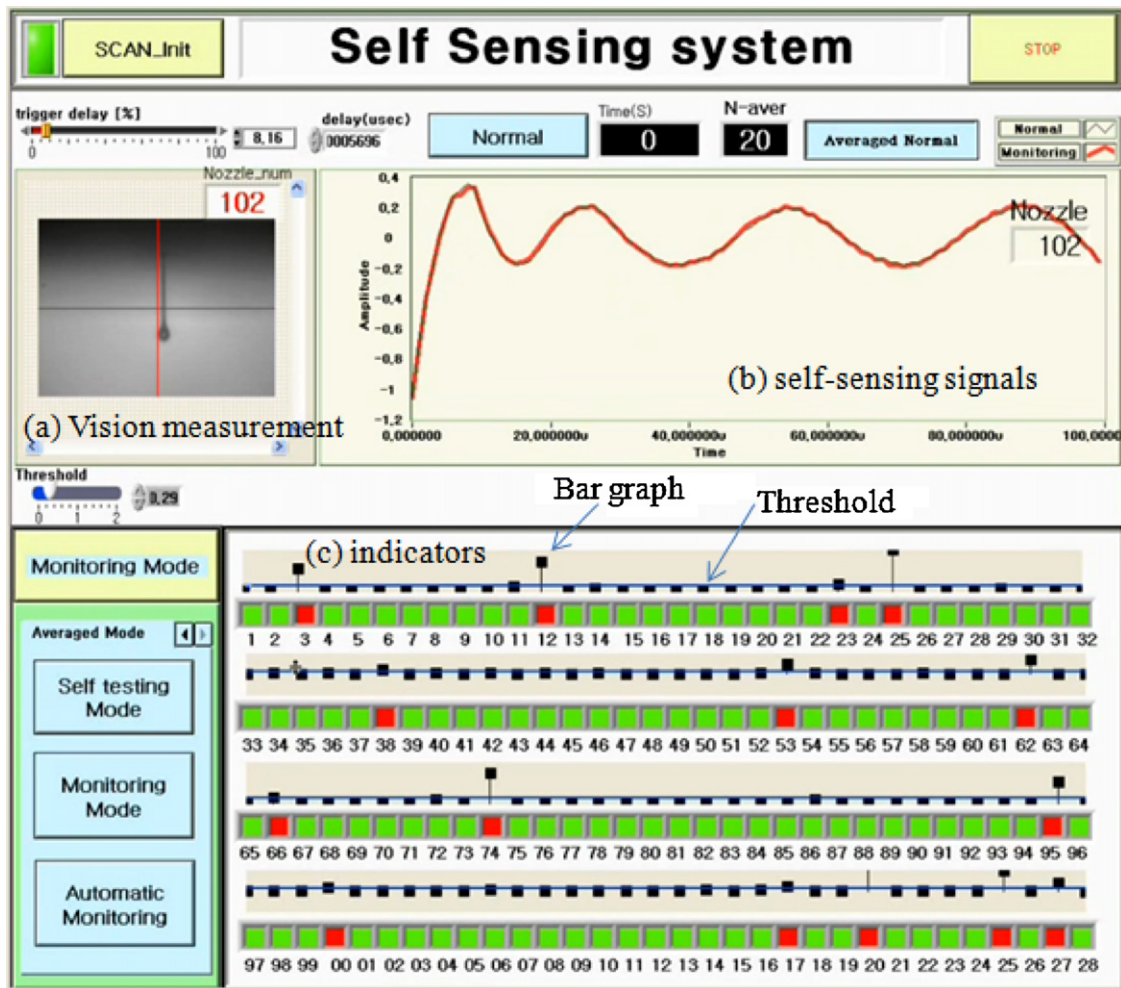


Fig. 14. Nozzle status when nozzle number of 102 was selected.

based on a target jetting speed. We can subsequently understand which nozzles are operating under normal jetting conditions. The self-sensing signals measured from nozzles with normal jetting conditions are used as reference data. For this purpose, software was developed that can scan the whole nozzle automatically to measure the jetting speed of each nozzle and the corresponding self-sensing signal, as shown in Fig. 13. This process took a few minutes because visual measurement was involved. In the event that a vision measurement system is not available in a printing system, other approaches can be used to define reference signals. For example, a test pattern can be printed on a substrate, and the printed pattern can be examined to determine if a nozzle is normal.

Once the reference data for each nozzle is saved, it is compared with the self-sensing signals to detect possible malfunctions. For this purpose, software was developed to determine the jetting status of a multi-nozzle head and to show the monitoring results such that each nozzle's status can be understood at a glance. In this study, arrays of color indicators were used to understand the status of entire nozzles. Also, the value of V_k , which was calculated using Eq. (8), was displayed as a bar graph for easy understanding of the extent of malfunction. The value of V_k was compared with the threshold value (the horizontal line across the bar graph) to judge the jetting status. If the value was higher than the threshold, then the nozzle was classified as a malfunction nozzle. The nozzle status can be easily understood from the nozzle classification using colored indicators (green: normal, red: abnormal) as shown in Fig. 14. However, there is a possibility of misclassification. For example, if

the graph value is slightly higher than the threshold value, the status is classified as a malfunction (red colored indicator) even though the jetting status may be acceptable. To avoid possible misclassifications, the bar graph can be used to understand the severity of the malfunction.

Another feature of the developed software is to confirm the self-sensing results by comparison with vision results. If the color indicator of a nozzle is selected by mouse click, then the position of the motion stage is controlled to measure the jetting behavior of the nozzle using a CCD camera. Here, the jetting signal and LED light are synchronized to obtain a frozen droplet image [10]. The visual jetting status image was acquired for the verification of self-sensing signals, and might not be required in an actual inkjet-based manufacturing system. Also, the self-sensing signals of the reference signal and monitoring signal of the selected nozzle were overlaid on the graph for the comparison with the vision image.

Figs. 14 and 15 show the captured screen images when a head containing abnormal jetting nozzles was monitored. Figs. 14(c) and 15(c) show the monitoring results indicating that there are abnormal jetting nozzles (red-colored indicators). The malfunctioning nozzles may be returned to normal jetting conditions after proper maintenance including purging and wiping. For detailed information about a specific nozzle, the corresponding colored indicator can be selected via mouse click to understand the self-sensing signal behavior and the droplet image behavior of the selected nozzle. For example, Fig. 14(a) and (b) shows a comparison of the vision-based measurement method and self-sensing

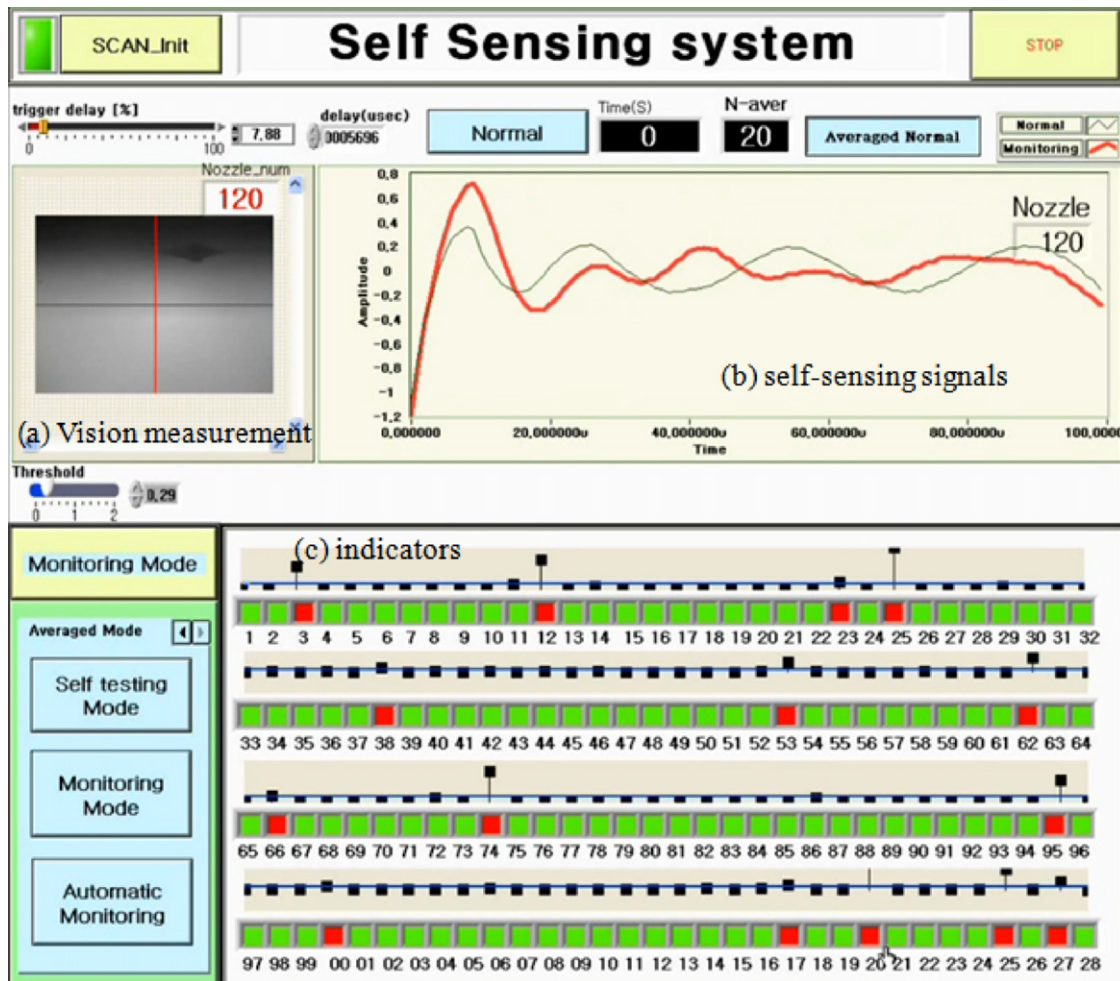


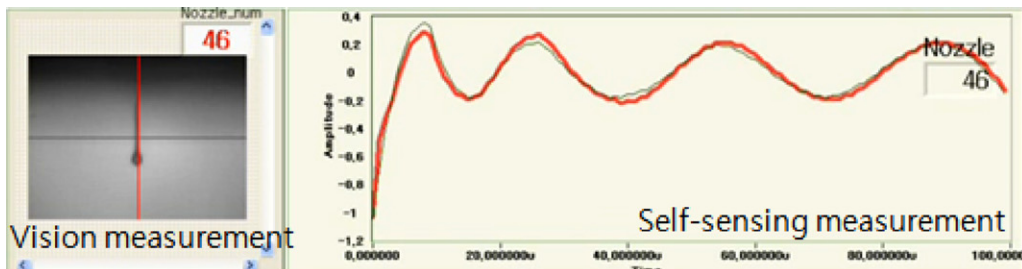
Fig. 15. Nozzle status when nozzle number of 120 was selected.

signal when the green color indicator of nozzle 102, which is classified as a normal nozzle by self-sensing monitoring, was selected. As seen in the droplet image of nozzle 102 in Fig. 14(a), we confirmed that the jetting condition was normal. Also, the monitored signal of nozzle 102 is quite similar to the reference signal as shown in Fig. 14(b). Here, the signals plotted using a thick line are monitored signals, and the thin line represents the reference signal. The signals shown in Fig. 14(b) were filtered to remove low frequency and high frequency noise from the acquired output voltage of the detection circuit. As a result, the signal appears to be different from the measured signal shown in Fig. 11. On the other hand, Fig. 15(a) and (b) shows the vision image and self-sensing signal of nozzle 120 when the red colored indicator of 120 was selected. Here, the monitored signals (thick line) of the nozzle differ significantly from the reference signals (thin line) in terms of magnitude and phase. The vision image shown in Fig. 15(a) verifies the monitored results since no droplet image was observed in the acquired image.

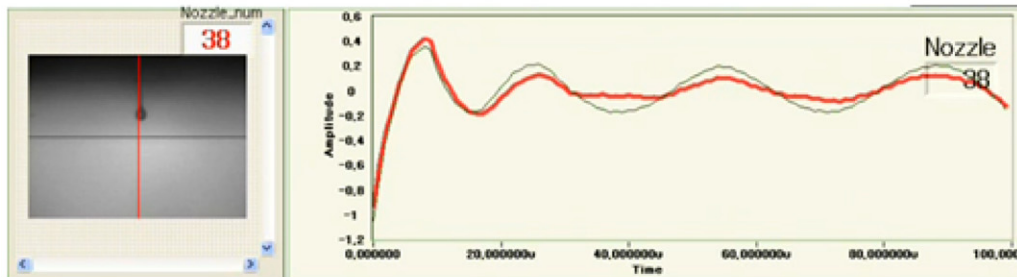
For a better understanding of the capabilities of the self-sensing signal to detect a malfunction, the jetting images and corresponding self-sensing signals typically observed in practice are shown in Fig. 16. To compare the droplet jetting performance of all nozzles, the trigger delay for the LED light with respect to the jetting signal was set at about 80 μ s. Theoretically, all droplets should appear at the same location in the acquired images if the jetting status of all nozzles is normal and the jetting speeds of all nozzles are the same. Otherwise, it can be concluded that the jetting condition of the corresponding nozzle deviated from the normal conditions. In this

way, we can understand the severity of a nozzle failure by observing the deviation of the jetting image location from the reference droplet image location. For example, the jetting image in Fig. 16(b) and (c) indicates that the jetting speed is smaller than the normal jetting condition shown in Fig. 16(a). Note that the reduced jetting speed shown in Fig. 16(b) may not be a serious condition and can be classified as normal jetting depending on the droplet accuracy required. However, Fig. 16(d) indicates that there was no jetting from nozzle 12, which requires corrective maintenance. As seen in the self-sensing signals shown in Fig. 16, the sensing signals are sensitive to jetting status such that the system can detect a serious non-jetting condition (nozzle 12) as well as a slightly changed jetting status such as low jetting speed. The severity of the abnormality can be measured using the value of V_k defined in Eq. (8). Experimentally, nozzles with normal jetting speed had values of less than 0.25. The value of V_k increased if the jetting behavior varied from normal jetting conditions as shown in Fig. 16(b) and (c). Here, the V_k of nozzles with low jetting speed ranged from 0.6 to 6. In case of non-jetting conditions as seen in Fig. 16(d), the value further increased. In this experiment, the threshold value of 0.29 is used such that nozzles having V_k higher than 0.29 can be classified as abnormal. Note that the threshold value was selected based on the experimental results observing the value of V_k according to jetting conditions. The threshold values should differ according to the printheads, drive electronics, circuit gain and ink properties.

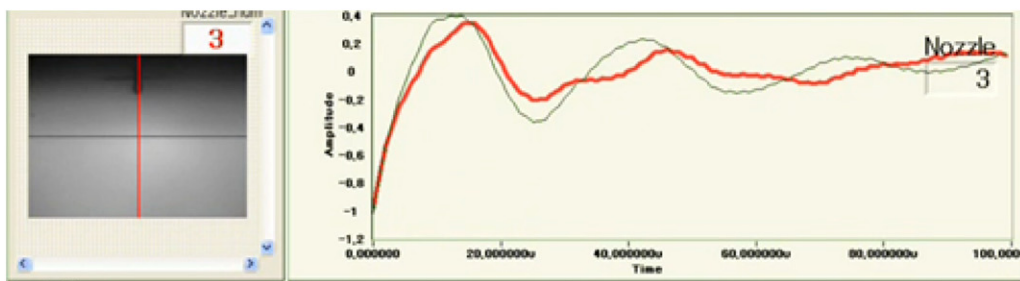
Note that the reference signals from an odd nozzle (nozzle number 3) are different from the signals from even nozzles (numbers 46,



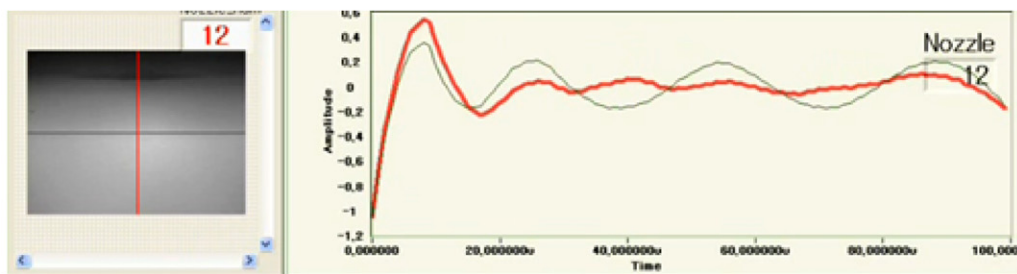
(a) Normal jetting nozzle (nozzle number 46).



(b) Reduced jetting speed (nozzle number 38)



(c) Reduced jetting speed (nozzle number 3)



(d) Non-jetting nozzle (nozzle number 12).

Fig. 16. Comparison of vision results and self-sensing signals.

38 and 12) because different drivers for odd and even nozzles were used. Also, it is difficult to perfectly balance a differential circuit in order to remove nominal signals that are unrelated to self-sensing signals.

For a better understanding of the proposed method and the current status of the monitoring module, a website video clip is referenced in [17].

4. Conclusions

To monitor the jetting conditions of a multi-nozzle head via piezo self-sensing, many technical problems must be solved: (1) the electrical noise in measured signals must be removed; (2) monitoring time should be minimized; (3) reference

self-sensing signals of each nozzle should represent normal jetting conditions to detect malfunctions; (4) the software should show the monitoring results in an effective way; and (5) the cost of implementing a monitoring system should be reasonably low. To solve these technical problems, we developed a low cost and high speed monitoring system that gives the monitoring results in less than 2 s when scanning 128 nozzles. The detection time could be reduced further with the help of faster computers.

To obtain better detection accuracy, the measured signals were averaged, and the signals were filtered in the frequency domain to suppress electrical noise. The vision comparison shows that the proposed scheme effectively detected a substandard jetting nozzle as well as a non-jetting nozzle.

Methods for measuring the statistical percentage of detection accuracy and long term reliability are being developed and tested for proposed technology to be used in inkjet-based manufacturing systems for large area displays.

References

- [1] D. Allbertalli, Gen 7 FPD inkjet equipment development status, in: Proceedings of SID (Society for Information Display), Boston, USA, May 22–27, 2005.
- [2] H.S. Koo, M. Chen, P.C. Pan, LCD-based color filter films fabricated by a pigment-based colorant photo resist inks and printing technology, *Thin Solid Film* 515 (3) (2006) 896–901.
- [3] D. Redinger, S. Moles, S. Yin, R. Farschi, V. Subramanian, An ink-jet-deposited passive component process for RFID, *IEEE Transactions on Electron Devices* 51 (12) (2004) 1978–1983.
- [4] K.S. Kwon, Methods for detecting air bubble in piezo inkjet dispensers, *Sensors and Actuators A* 153 (1) (2009) 50–56.
- [5] J.D. Jong, G.D. Bruin, H. Reinten, M.V.D. Berg, H. Wijshoff, M. Versluis, D. Lohse, Air entrapment in piezo-driven inkjet printheads, *Journal of Acoustical Society of America* 120 (3) (2006) 1257–1265.
- [6] J.M.M. Simons, M.A. Groninger, Printing Apparatus, European Patent, EP 1 013 453 A2 (2000).
- [7] B.H. Kim, T.G. Kim, T.K. Lee, S. Kim, S.J. Shin, S.J. Kim, S.J. Lee, Effect of trapped air bubbles on frequency responses of the piezo-driven inkjet printhead and visualization of the bubbles using synchrotron X-ray, *Sensors and Actuators A* 154 (1) (2009) 132–139.
- [8] K.S. Kwon, J.K. Go, D.S. Kim, Methods for detecting jetting failure of inkjet dispensers, Kentucky, USA, September, Proceedings of NIP25 and Digital Fabrication (2009).
- [9] B.L. Lee, S.I. Kim, Piezo-driven inkjet printhead monitoring system, *Journal of Korean Sensors Society* 19 (2) (2010) 124–129 (in Korean).
- [10] K.S. Kwon, Speed measurement of ink droplet by using edge detection techniques, *Measurement* 42 (1) (2009) 45–50.
- [11] K.S. Kwon, Waveform design methods for piezo inkjet dispensers based on measured meniscus motion, *Journal of Microelectromechanical Systems* 18 (5) (2009) 1118–1125.
- [12] J.D. Jong, R. Jeurissen, H. Borel, M.V.D. Berg, H. Wijshoff, H. Reinten, M. Versluis, A. Prosperetti, D. Lohse, Entrapped air bubbles in piezo-driven inkjet printing: their effect on the droplet velocity, *Physics of Fluids* 18 (12) (2006) 121511.
- [13] R. Jeurissen, J.D. Jong, H. Reinten, M.V.D. Berg, H. Wijshoff, M. Versluis, D. Lohse, Effect of an entrained air bubble on the acoustics in an ink channel, *The Journal of the Acoustical Society of America* 123 (5) (2008) 2496–2505.
- [14] D.B. Bogy, F.E. Talke, Experimental and theoretical study of wave propagation phenomena in drop-on-demand ink jet devices, *IBM Journal of Research and Development* 28 (3) (1984) 314–321.
- [15] K.S. Kwon, W. Kim, A waveform design method for high speed inkjet printing based on self-sensing measurement, *Sensors and Actuators A* 140 (2007) 75–83.
- [16] K.S. Kwon, Laboratory Developed Printing System, 2010, Available from: <http://www.youtube.com/watch?v=iNc-skHODcA>.
- [17] K.S. Kwon, Inkjet Monitoring System Development, 2011, Available from: <http://www.youtube.com/watch?v=qnnNt7GrWdw>.

Biographies

Kye-Si Kwon is an associate professor at Soonchunhyang University in Korea in the department of mechanical engineering. He received his BS degree in mechanical engineering from Yonsei University, Seoul, Korea in 1992. He holds a master's degree (1994) and a PhD (1999), both in mechanical engineering from KAIST, Korea. Before joining Soonchunyang University, he was a member of the research staff at the Samsung Advanced Institute of Technology. His current work is focused on the development of measurement methods for controlling inkjet head.

Yun-Sik Choi is a master student at Soonchunhyang university in the department of mechanical engineering.

Dae-Yong Lee is a master student at Soonchunhyang university in the department of mechanical engineering.

Jeong-Seon Kim is an engineer at SEMES. He is in charge of developing inkjet based manufacturing system for large flat panel display.

Dae-Sung Kim is a senior engineer at SEMES. He is in charge of developing inkjet based manufacturing system for large flat panel display.